pendent of θ, indicating an equal distribution of emitted radiation.

References

[1] MacNaughton, J. D., "Unfurlable Metal Structures for Spacecraft," *Canadian Aeronautics and Space Journal*, Vol. 9, No. 4, 1963, pp. 103–116.

[2] Grimshaw, E. R. and Wells, A., "Gravity Gradient Booms—Their Origin and Evolution," Dec., 1968, Symposium on Gravity Gradient Attitude Control, Sponsored by the Air Force (SAMSO) and Aerospace Corporation, Los Angeles, Calif.

[3] Kreith, F., "Radiation Heat Transfer," International Textbook, Scranton, Pa., 1962, pp. 40–42, 50–51.

Effect of Reflections from CO_2 Cryodeposits on Thermal Testing in Space Chambers

D. W. Mills Jr.* and A. M. Smith†
ARO Inc., Arnold Air Force Station, Tenn.

In space simulators the test vehicle is surrounded by black surfaces which are cooled to near 77°K to minimize their emitted radiant flux and to increase the vacuum pumping capacity of the space chamber. If CO_2 or H_2O cryodeposits form on the black cryopanels, their visible and near-infrared reflectance properties are altered.[1] This Note presents the results of an experiment investigating the effect of reflections from CO_2 cryopanel deposits on the steady-state temperatures of a test article irradiated directly by a simulated solar flux of 140 mw/cm².

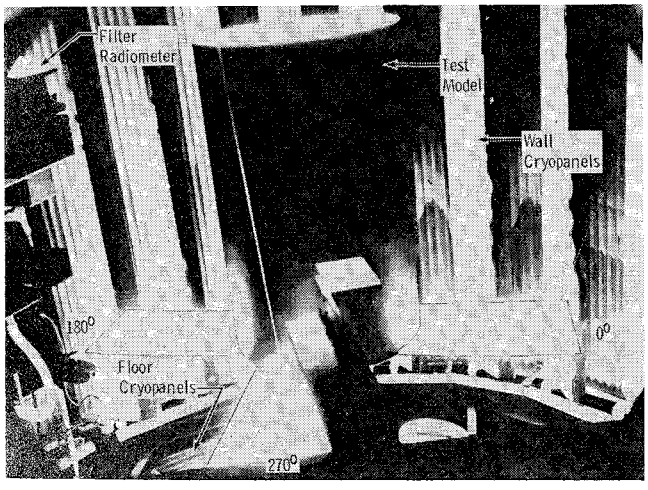

Fig. 1 Hollow cylinder-paddlewheel test model mounted in space simulation chamber showing CO_2 cryodeposits on wall and floor cryopanels.

Presented as Paper 69-1012 at the AIAA/ASTM/IES 4th Space Simulation Conference, Los Angeles, Calif., September 8–10, 1969; submitted October 20, 1969; revision received December 15, 1969. This work was sponsored by the Arnold Engineering Development Center, Air Force Systems Command, under Contract F40600-69-C-0001 with ARO Inc. The tests reported here were carried out in cooperation with the Institut für Raumsimulation, Deutsche Forschungs-und Versuchsanstalt für Luft-und Raumfart, Porz-Wahn, West Germany.

* Research Engineer, Thermal Physics Section, Aerospace Environmental Facility. Associate AIAA.

† Supervisor, Thermal Physics Section, Aerospace Environmental Facility and Associate Professor of Aerospace Engineering (Part-time), University of Tennessee Space Institute, Tullahoma, Tenn. Member AIAA.

The space chamber employed was a vertical cylindrical tank, 12 ft in diameter by 35 ft in height. Its vacuum pumping system consisted of mechanical and oil diffusion pumps, and LN_2-cooled cryopanels. The chamber was equipped with an off-axis, "top sun" solar simulator whose radiation source was an array of 20-kw, short-arc xenon lamps. After passing through an optical integrator, the radiation was reflected downward by a 10-ft-diam collimating mirror to irradiate an 8-ft-diam by 8-ft-deep test volume at one Earth orbit solar constant.

The test article was a closed hollow cylinder with flat paddle surfaces attached to one end (see Fig. 1). This configuration was constructed from 0.125-in.-thick 2024 T4 aluminum sheet and instrumented with copper-constantan thermocouples at the 21 locations shown in Fig. 2. The test model was oriented in the space chamber so that the longitudinal axis of the cylinder was parallel to the collimated beam of solar simulator irradiance. The azimuthal orientation of the model was such that the $\varphi = 270°$ index position (see Figs. 1, 2) faced the chamber viewports. It is seen from Fig. 1 that the top surfaces of the cylinder and paddles, which were irradiated directly by the solar simulator, were coated with white paint. The circumferential surface of the cylinder and the underside of the cylinder and paddles were coated with black paint.

Procedure

The chamber was first evacuated to 10^{-5} torr using mechanical and oil diffusion pumps. Then the cryopanels were cooled with LN_2 thereby surrounding all but the top of the test volume with black 77°K surfaces. After the chamber pressure had decreased to 10^{-6} torr, the solar simulator irradiance was set at 140 mw/cm². The test model was irradiated until its temperatures reached steady-state after 3.1 hr. Readings from the 21 thermocouples on the model were recorded periodically during this time. The solar simulator irradiance was monitored by a filter radiometer (see Fig. 1) and a calibrated thermopile mounted in the chamber at the model level.

After this test run was completed, the solar simulator was turned off and the wall cryopanels were allowed to warm but the floor cryopanels were maintained near 77°K. The conventional pumping system was then valved off and a known quantity of CO_2 was introduced diffusely into the chamber. This formed a given thickness cryodeposit on the floor cryopanels and altered their reflectance. The thickness of CO_2 deposited on the floor cryopanels was determined from

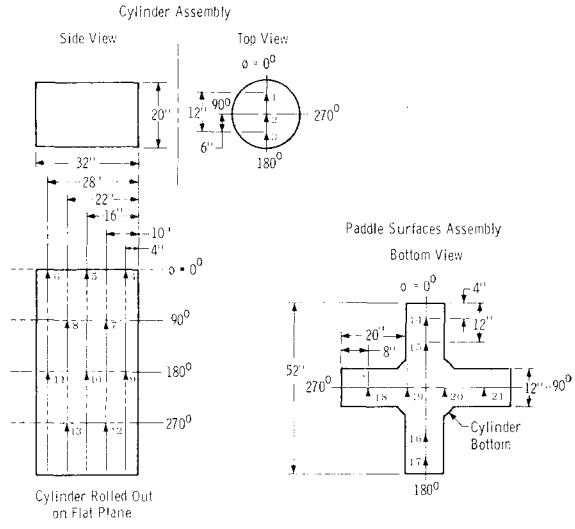

Fig. 2 Thermocouple locations on test model.

mass conservation principles using a density of 1.5 g/cm³ for solid CO_2.[1] After the CO_2 cryodeposit had been formed, the vacuum pumping system was reopened and the chamber pressure was reduced to 10^{-6} torr. Then, the wall cryopanels were cooled to 77°K and the solar simulator irradiance set at 140 mw/cm². All 21 temperatures on the test model were recorded periodically until steady-state conditions were attained. The procedure was then repeated for cryodeposit thicknesses up to and including 127 μ. A slightly different approach was employed for deposit thicknesses from 0.146 through 2.51 mm. The wall cryopanels were not warmed up while CO_2 was being added to the chamber and thus the CO_2 cryodeposit formed on both the wall and floor cryopanels.

Results and Discussion

The model steady-state temperatures for one solar constant irradiance with negligible CO_2 deposit on the cryopanels were measured at 21 locations and are given in Fig. 3. These data are displayed along the model surface for the four azimuthal planes $\varphi = 0°$, 90°, 180°, and 270°. It is seen from Fig. 3 that the paddle surfaces and cylinder top irradiated directly by the solar simulator are the highest temperature areas on the model with the former being somewhat hotter due to their additional absorption of solar simulator flux reflected from the floor cryopanels. Figure 3 also indicates that the lowest temperature area on the model surface occurs around the center of the cylinder side. It is also seen in Fig. 3 that the model temperatures at corresponding locations in the $\varphi = 0°$ and $\varphi = 180°$ azimuthal planes are essentially identical but those in the $\varphi = 90°$ and $\varphi = 270°$ planes are not. The temperaures of the cylinder side area and paddle surface in the $\varphi = 90°$ plane are appreciably lower than the corresponding temperatures in the $\varphi = 270°$ plane. This is because both the cylinder side area and the top of the paddle surface in the $\varphi = 270°$ azimuthal plane absorb 295°K infrared radiation coming from the viewport windows while the cylinder side area and paddle surface in the $\varphi = 90°$ plane are not exposed to infrared radiation from viewport windows.

Figure 4 gives the total normal reflectance of various thicknesses of CO_2 cryodeposit on a black paint substrate for a spectral irradiance equal to that of the solar simulator.[2] The reflection reduction phenomenon observed for deposit thicknesses less than 100 μ has been reported previously[1] and is due to the refractive index of the deposit being less than that of the black paint. If this decrease in reflectance occurred for the floor cryopanels when thin CO_2 deposits were present then the solar simulator flux reflected to the test model would be reduced. The results given in Fig. 5a show that for thin deposits of less than 95 μ thickness the reduction in solar simulator flux reflected to the test model is significant enough to cause a decrease in the steady-state temperatures of the model. Data are presented for four representative model locations; the cylinder top (thermocouple location 2), the cylinder side (thermocouple location 5), the paddle surface (thermocouple location 18), and the cylinder bottom (thermocouple location 20). The maximum temperature decrease observed on the paddle surface is 5°F, on the cylinder bottom, 3.5°F, and on the cylinder side, 3°F. These maximum temperature decreases occur for a deposit thickness of 17 μ. It is also seen that there is a small decrease in the temperature on the cylinder top. This temperature decrease is not directly attributed to a reduction in solar simulator flux reflected to the cylinder top but is a result of the increase in energy flux loss from the top by conduction and internal radiation to the colder cylinder side and bottom.[3]

Further analysis of the results in Fig. 5a shows that when the CO_2 deposit thickness on the floor cryopanels exceeded

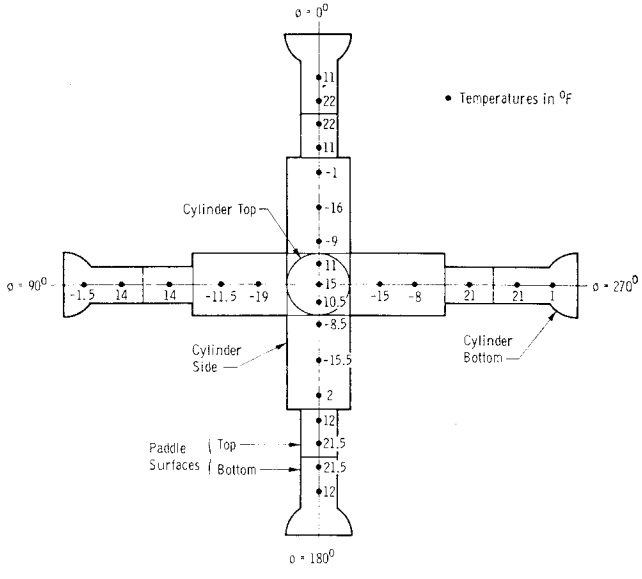

Fig. 3 Test model steady-state temperatures for one solar constant irradiance with no CO_2 deposits on space simulation chamber cryopanels.

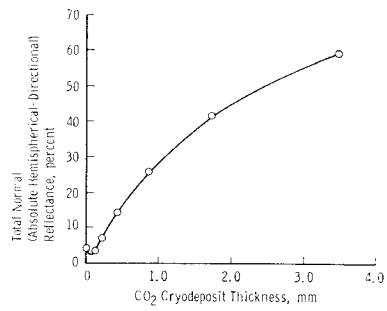

Fig. 4. Total normal reflectance of various thicknesses of CO_2 cryodeposit on a black paint substrate for irradiance from test chamber xenon arc solar simulator.

a) Thin deposits

b) Thick deposits

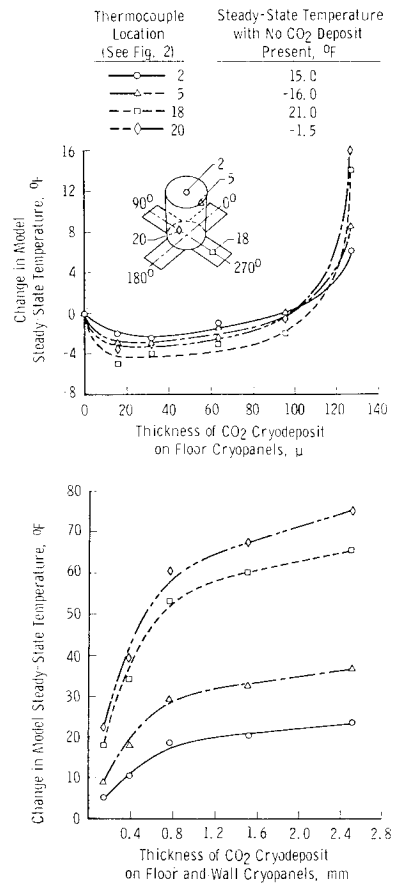

Fig. 5 Changes in steady-state temperatures of test model due to reflection of solar simulator flux from CO_2 cryodeposits.

approximately 105 μ the model temperatures at the four locations were greater than when no CO_2 cryodeposits were present. Figure 4 shows that this is to be expected since the reflectance of CO_2 deposit on a black paint substrate is greater than the reflectance of the bare substrate when the deposit thickness exceeds approximately 100 μ. For a deposit thickness of 127 μ, the temperature increases resulting from the increased solar simulator flux reflected to the model are, as seen in Fig. 5a, 16°F on the cylinder bottom, 14°F on the paddle surface, and 8.5°F on the cylinder side. The 6°F temperature increase observed on the cylinder top is a result of the decrease in the energy flux loss from the cylinder top by conduction and internal radiation to the cylinder side and bottom.

Figure 5b presents the changes in the steady-state temperatures obtained at the four representative locations on the test model due to reflection of solar simulator irradiance from various thicknesses of thick (0.146 to 2.51 mm) CO_2 deposits on the floor and wall cryopanels. The changes in the four temperatures rise drastically with thickness due to the increased reflection of solar simulator irradiance by the thicker CO_2 cryodeposits. The greatest increases in temperature with deposit thickness occur on the cylinder bottom and the paddle surface since these two representative model locations have the largest view factor for the solar simulator irradiance reflected directly back toward the vehicle from the floor cryopanel deposits. At location 20 on the cylinder bottom, this temperature increase is as much as 75°F for a deposit thickness of 2.51 mm. Most of this temperature increase, 60°F, occurs for a thickness of 0.78 mm. Figure 5b also shows that a smaller temperature increase occurs at location 5 on the cylinder side (up to 37°F for a 2.51 mm deposit) than on the cylinder bottom and paddle surface locations because the former location does not have a large view factor for the solar simulator irradiance reflected from the floor cryopanel deposits. However, location 5 on the cylinder side does have a large view factor for solar simulator flux reflected from the wall cryopanel deposits. In addition, part of the temperature rise at this location results from an increase in the conduction and radiant energy flux from the cylinder bottom and paddle surface which have an increasingly higher temperature. The smallest temperature rise observed on the model (up to 24°F for 2.51 mm deposit) was at location 2 on the cylinder top. Since the cylinder top is highly reflecting in the spectral range of the solar simulator and also has only a small view factor for solar simulator flux reflected from the wall cryopanel deposits, most of the temperature increase occurring at this location is due to the decrease in the energy flux loss from the cylinder top by internal radiation to the cylinder side and bottom.

Conclusions

The reflection of solar simulator flux from CO_2 cryopanel deposits less than 100 μ thick has only a small effect on the thermal balance of a test article in a space chamber. This effect is not detrimental and the steady-state temperatures of the test vehicle can actually be lower than when there are no CO_2 deposits on the chamber cryopanels. The reflection of solar simulator flux from CO_2 cryopanel deposits of thicknesses greater than 100 μ has a very adverse effect on the thermal balance results for a test model in a space chamber. Most of the increase in test model steady-state temperatures occurs for a deposit thickness of only 0.78 mm.

References

[1] Wood, B. E. and Smith, A. M., "Spectral Reflectance of Water and Carbon Dioxide Cryodeposits from 0.36 to 1.15 μ," *AIAA Journal*, Vol. 6, No. 7, July 1968, pp. 1362–1367.

[2] Seiber, B. A., private communication, July 1969, ARO Inc.

[3] Hsia, H. M., private communication, July 1969, ARO Inc.

Interior Ballistics for Wide-Temperature Throttling of Solid-Propellant Rockets

R. L. H. Lou*

Aerojet-General Corporation, Sacramento, Calif.

Introduction

CONTROLLABLE mass flow rate, or throttling, over a wide temperature range, is one of the principal goals in the current effort to improve the performance and versatility of solid-propellant rockets. To minimize inert weight, the required throttling ratio, $\tau_{req} \equiv (\dot{m}_{max}/\dot{m}_{min})_{req}$ should be accomplished in as low a chamber pressure ratio, $\phi \equiv (P_{max}/P_{min})$, as possible. This, in turn, requires a high burning rate pressure exponent, n, which is limited only by the capability of the control system. Generally, $0.7 \leqslant n \leqslant 0.8$ is considered optimum. For wide-temperature-range operations, typically −65 to 165°F, the temperature sensitivity of equilibrium pressure π_K can significantly increase the pressure ratio required. Thus, π_K should be minimized.

This Note concerns the interior ballistic considerations pertinent to wide-temperature-range throttling by means of a variable-throat-area nozzle. Specifically, the discussion delineates a) the effect of the operating temperature range on the usable throttling ratio, $\tau_u \equiv (\dot{m}_{max}/\dot{m}_{min})_{usable}$, b) the specific temperature/pressure combinations that limit τ_u (and the combinations that do not), and c) the tradeoff between pressure and temperature sensitivity. It is shown that a single parameter, designated the wide temperature throttling exponent, n_T, is useful for rapid screening of the effects of propellant composition and on throttling potential.

Discussion

For simplification and clarity, it is assumed that the pressure and temperature sensitivities of the discharge coefficient are negligible, and that the propellant ballistics can be represented by

$$r = ce^{\pi_p(\Delta T)}P^n \tag{1}$$

at the design temperature, even though these assumptions are not essential to the basic concept advanced. c is an empirical constant whereas T is propellant temperature. Thus, π_K, π_p and n are related by the well known expression:

$$\pi_K = \pi_p/(1 - n) \tag{2}$$

where

$$\pi_K = \left[\frac{\partial \ln p}{\partial T}\right]_K \quad \begin{array}{l}\text{(temperature sensitivity of pressure at}\\ \text{constant } K\text{, propellant burning surface}\\ \text{area to throat area ratio)}\end{array} \tag{3}$$

$$\pi_p = \left[\frac{\partial \ln r}{\partial T}\right]_P \quad \begin{array}{l}\text{(temperature sensitivity of burning rate}\\ \text{at constant pressure)}\end{array} \tag{4}$$

Equation (2) shows that π_K can be reduced by reducing n and/or π_p. Since reducing π_K by reducing n would only lead to a net loss in τ_u for a given ϕ, the only useful approach to reduce π_K for wide temperature throttling is to reduce π_p. A usable throttling ratio (τ_u) for a wide temperature range is the one throttling ratio that can be realized at every point within the temperature range. It is the throttling ratio obtainable at a given temperature (for a given pressure ratio and n) diminished due to the effect of π_p. Furthermore, it will be shown later that only the reductions in π_p at the high T/low P

Received September 11, 1969; revision received December 8, 1969.

* Program Manager, Advanced Technology Programs, Propellant Research and Development Department. Member AIAA.